Bulgarian Chemical Communications, Volume 52, Special Issue E (pp. 41 - 48) 2020

Electrochemical polymerization and in situ characterization of PANI in presence of chemically modified graphene

A. Petrovski[1], P. Perica Paunović*[1], A. Grozdanov[1,2], A. T. Dimitrov[1], I. Mickova[1], G. Gentile[2], M. Avella[2]

[1]*Faculty of Technology and Metallurgy, Ss Cyril and Methodius University, RudjerBošković, 16, 1000 Skopje, R. Macedonia*

[2]*Institute for Chemistry and Technology of Polymers, National Research Council, Fabricato Olivetti 70, Pozzuoli, Napoli, Italy*

Received October 27, 2019; Accepted January 21, 2020

The subject of this research is in situ study of the process of polyaniline (PANI) electro-polymerization in the presence of graphene. The Graphene was firstly purified/chemically modified, and then SEM/EDS analysis was performed in order to characterize the material. These results have shown that purification and chemical modification of the graphene, leads to formation of some complex groups which is good for interaction with polymers and formation of nanocomposites. In order to determine the conditions for electro-polymerization of aniline to PANI in the presence of graphene, electrochemical characterization was performed by means of cyclic voltammetry (CV) and steady state polarization (SS).The influence of different scan rates (10, 20, 50 and 100 $mV.s^{-1}$) was examined during the process of electro-polymerization and the double layer capacity of pure PANI (1.75 $mF.cm^{-2}$) and nanocomposite with graphene (121.07 $mF.cm^{-2}$) was calculated. The influence of the type of CNSs, different mass fractions (1%, 2%, 3% and 10 % wt. graphene vs. PANI) and two different pathways of introduction of graphene in PANI matrix on the electro-polymerization rate were analyzed. According to these results, it is confirmed that graphene acts as an incipient in the process of electro-polymerization and improves the electrical conductivity and the double layer capacity of PANI, which is suitable for various fields of applications of this nanocomposite.

Keywords: Electro-polymerization, polyaniline (PANI), graphene, cyclic voltammetry (CV), steady state polarization (SS)

INTRODUCTION

Within the conductive linear-backbone polymers such as polyacetylene, polypyrrole, polyindole and their copolymers, PANI shows the greatest attraction to the scientific community. It possesses unique properties such as good environmental stability, easy and low cost synthesis, electrical and electrochemical properties such as electrical conductivity, electrochemical activity, and possibility to adjust these properties during the synthesis and doping processes [1-3]. PANI can exist in five redox states, from which emeraldine base is the only electrical conductive form [4, 5], when is converted in emeraldine salt. PANI is appropriate for various fields of applications such as energy storage devices, electrochromic devices, supercapacitors, sensors etc. [4-6]. However, its application is constrained by some disadvantages such as poor mechanical properties and low process ability. Due to the nature of this polymer, it is very difficult to overcome these disadvantages and presents a big challenge to the scientific community. Different approaches have been tried to make PANI soluble; to obtain PANI suitable for processing in its liquid state; to adjust its electrical conductivity during the doping process and researches have been done about the impact of the humidity on this properties [5-11]. All these researches show some promising results, but there are still some of its disadvantages left to explore.

One of the next steps in improving the applications of PANI is obtaining of PANI with grapheme nanocomposites. One of PANI's useful properties is the interaction with polymers and forming of nanocomposites. PANI/graphene nanocomposites can be prepared using direct mixing methods, chemical or electrochemical polymerization [12]. All of these methods have their own advantages and disadvantages, but electrochemical polymerization has shown the best results in order to obtain pure PANI form without some residuals of the other redox states, which can affect the properties of the nanocomposite. This method is appropriate for direct electro-polymerization of the nanocomposites on screen printed electrodes with the possibility to control the thickness of the film and to control its properties, which is extremely useful for applications in electronics, electrochemical devices, sensors etc. [13].

* To whom all correspondence should be sent.
E-mail: pericap@tmf.ukim.edu.mk

© 2020 Bulgarian Academy of Sciences, Union of Chemists in Bulgaria

In order to obtain good interfacial interactions between graphene and PANI, several authors propose previous functionalization of the graphene's surface in order to form some functional groups which are suitable for interaction with PANI, and therefore, the formation of stable nanocomposite [14, 15].

This work is done in order to characterize PANI/graphene nanocomposites using in situ electrochemical measurements in the process of electro-polymerization of PANI in the presence of graphene.

2. EXPERIMENTAL

2.1. Materials

For the experiments in this paper, aniline, sulfuric acid (H_2SO_4), nitric acid (HNO_3), hydrogen peroxide (H_2O_2), hydrogen fluoride (HF) and distillated water were used. The chemicals were supplied by Sigma Aldrich. All chemicals had p.a. purity, except the aniline which was purified by distillation. The graphene used was produced in the laboratory of the Faculty of Technology and Metallurgy in Skopje by exfoliation during molten salts electrolysis [16].

2.2. Purification and preparation of chemically modified graphene

For further use, the graphene was purified and then modified by standard procedures [17, 18]. The procedure comprises dispersing 10 g graphene nanoparticles in 300 ml distilled water and then exposing the dispersion to ultrasound for 30 minutes. After that, concentrated H_2O_2 was added to the dispersion to be used a 10 % solution and was stirred by magnetic stirrer for 2 h with 900 rpm. The dispersion was filtered through vacuum filter and the solid fraction was washed several times with boiled distilled water and with cold distilled water at the end. Further, the solid fraction was dispersed in concentrated solution (49 %) of HF, and after 1 h was filtered and washed as before. With this procedure, graphene was purified from some of the residuals such as unexfoliated graphite and some inclusions from the production process [16]. This was confirmed by SEM/EDS study. SEM observation was carried out by scanning electron microscope (SEM) FEI Quanta 200 using secondary electron detector and acceleration voltage of 30 kV.

In order to produce chemically modified graphene, purified graphene was treated with a mixture of concentrated H_2SO_4 and HNO_3 acids (volume ratio H_2SO_4 to HNO_3 was 3:1). Weight ratio of graphene to acid solution was 100:1. The dispersion was stirred by magnetic stirrer for 12 h at 50 °C to get acid modified graphene. After that, the solution was centrifuged at 5000 rpm. The solid fraction was washed with distilled water several times to purify graphene form acid residuals [18].

2.3. Electrochemical cell and instrumentation

The experiments were carried out in 250 ml three-electrode one-compartment glass cell. The working electrode was platinum tile with active surface of 10 cm^2 and a platinum grid was used as counter electrode. As a reference electrode Saturated calomel electrode (SCE) was used. The polymerization electrolyte consists of 0.1 M aniline dissolved in 0.5 M H_2SO_4.

The electrochemical characterization was performed by METROHM Autolab PGSTAT 128 N for CV and WENKING HC 500 for stationary polarizing investigations. All the experiments were carried out at room temperature.

3. RESULTS AND DISCUSSION

3.1. SEM/EDS analysis of graphene

Scanning electron microscopy was performed in order to study the graphene morphology and the effect of the purification/modification processes. Fig. 1 shows untreated graphene (Fig. 1-a), purified graphene by H_2O_2 and HF (Fig. 1-b) and chemically modified graphene by mixture of H_2SO_4 and HNO_3 (Fig. 1-c). As it can be seen, graphene flakes are with diameter from 1 to 20 μm. These variations of the diameter are attributed to the difficulty of controlling the interactions in the exfoliation process [19]. According to the literature [20], graphene shows high transparency from about 97.7 %. Xie and Spallas report [21] that it is impossible to count the flakes and analyze graphene layers using SEM, and this analysis is useful only for morphology investigations. According to this, analyzing the transparency of the graphene shown at Figure 1, one can conclude that there is a big variation of the number of layers into graphene flakes, but an accurate count cannot be done. Due to the transparency shown in Figure 1-a, there is a regions with unexfoliated graphite left in the material. The white dots left on the graphene flakes surface confirm this. Analyzing Figure 1-b, after treatment of the graphene with H_2O_2 and HF, there is no presence of white dots on the graphene flakes surface, and the transparency of the material is more uniform, which points out on efficient removal of the residuals from graphene. This is also confirmed with EDS, and the results are shown in Table 1.

Table 1. EDS analysis of graphene

	C	O	Na	Cu
Unreacted graphene	87.9	6.24	5.78	0.08
Graphene treated with H_2O_2 and HF	89.51	5.07	5.29	0.13
Graphene treated with H_2SO_4 and HNO_3	86.30	11.66	2.05	/

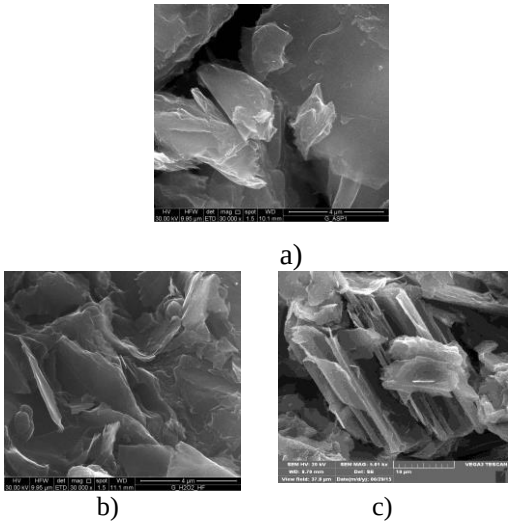

a) b) c)

Fig. 1. TEM images of a) as-prepared graphene, b) purified graphene by H_2O_2 and HF and c) chemically modified graphene by mixture of H_2SO_4 and HNO_3.

Purification of graphene, leads to wrinkled structure that causes sheet folding [22]. Treating the graphene with strong acid solutions such as concentrated H_2SO_4 and HNO_3, causes edges cutting and gives a more uniform form of the flakes. In the graphene flakes shown in Figure 1-c, oxidized edges can be seen, which can be attributed to the formation of some amide and carbamide groups with hydroxyl and carboxyl groups. This results in the disruption of sp^2 bonds, transforming them into sp^3 bonds. These transformed carbon centers results in the creation of electron-flow disruptions and the creation of an energy gap. In this way, the functionalization of multiple-layer graphene will change the electronic properties from near-metal into semiconducting [17,23]. These oxidized edges with formation of carboxyl and hydroxyl groups were also confirmed by EDS analysis. The results presented in Table 1, show that there is a great increase of oxygen in the material which points out that the chemical modification leads to the formation of these groups on its surface as well as to the complete removal of the residuals such as Na and Cu. On the other hand, the introduction of sulfur in the material leads to some complex groups with carboxylic groups being formed. These transannular interactions can cause polarization of the carboxylic groups [24], which is helpful for the whole interaction with polymers and formation of composites. Also, within this phenomenon proton removal from some components occurs [25], which is useful for the application of graphene in some electrochemical devices.

3.2. Cyclic voltammetry (CV)

Cyclic voltammetry was performed in order to determine the redox processes of the electro-polymerization of aniline to polyaniline. Cyclic voltammograms were scanned in the potential region of –0.2 to 1 V with and without presence of graphene. Shown on Fig. 2 are the CV spectra recorded for the following electrolytes: i) 0.1 M aniline + 0.5 M H_2SO_4 and ii) 0.1 M aniline + 0.5 M H_2SO_4 + graphene 3 % wt. related to the weight of aniline.

Both spectra show the same eight characteristic peaks related to the corresponding redox reactions characteristic for oxidation/reduction in the aniline/polyaniline system [26]. These peaks are more intense and very well pronounced for the electrolyte including graphene, in comparison with the corresponding peaks for the electrolyte containing 0.1 M aniline + 0.5 M H_2SO_4. Positions of the corresponding peaks are presented in Table 2.

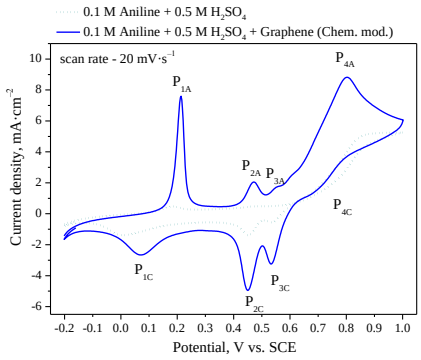

Fig. 2. Cyclic voltammograms of a) 0.1 M aniline + 0.5 M H_2SO_4 and b) 0.1 M aniline + 0.5 M H_2SO_4 + graphene 3 % wt. related to the weight of aniline.

Table 2 Position of characteristic peaks (V) registered by cyclic voltammetry.

Electrolyte	P_{1A}	P_{1C}	P_{2A}	P_{2C}	P_{3A}	P_{3C}	P_{4A}	P_{4C}
0.1 M Aniline + 0.5 M H_2SO_4	0.184	0.023	0.473	0.450	0.553	0.530	0.889	0.64 – 0.78
0.1 M Aniline + 0.5 M H_2SO_4 + Graphene (Chemically modified)	0.214	0.072	0.471	0.450	0.559	0.533	0.802	0.64 – 0.78

The first step of oxidation of aniline is denoted with P_{1A}. It is attributed to the transformation of leucoemeraldine (basic oxidation state of PANI - completely reduced) to emeraldine (oxidation state of PANI - half oxidized). P_{1C} in cathodic region is attributed to the reverse transformation. For both electrolytes, the position of the peaks P_{1A} and P_{1C} is at different potentials (Table 1), which points out on the irreversibility of this redox reaction. The next redox pair P_{2A}/P_{2C} corresponds to the formation of secondary by products like benzoquinone and hydroquinone [26], and this also leads to overoxidation and degradation of PANI [27]. The redox pair P_{3A}/P_{3C} is ascribed to the transformation of p-aminophenol to benzoquinonemine and vice versa [27, 28]. Also, these redox reactions are irreversible according to the positions of the anodic and corresponding cathodic peaks (Table 1). The last oxidation peak P4A, corresponds to the transformation of emeraldine oxidation state of PANI (half oxidized) to pernigraniline (completely oxidized state) [29, 30].

Due to the presence of carbon nanostructure in the electrolyte, the growth of the composite on the electrode is more intense. This can be attributed to higher electroconductivity and electroactivity of graphene that lead to faster electrons exchange between ions and the electrode [31]. Graphene also acts as a incipient in the system because of its large specific surface and accelerates the reaction rate.

The influence of the purification and modification of graphene on the reaction rate is shown on Fig. 3.

The presence of untreated graphene shows slightly higher current densities than those in the voltammogram of pure PANI. Purification of graphene causes further increase of the current densities related to the previous systems. The increase in current densities is more pronounced in cases where chemically modified grapheme is used.

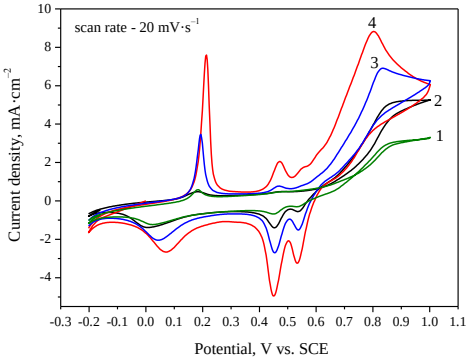

Fig. 3. Cyclic voltammograms of aniline in presence of chemically modified graphene (4), purified graphene (3), untreated graphene (2) and without presence of carbon nanostructure (1). Electrolyte: 0.1 M Aniline + 0.5 M H_2SO_4

This confirms the considerations from SEM/EDS analysis and shows that the purification and chemical modification of graphene leads to higher active surface area of the material and better electrical conductivity [31].

In order to determine the double layer capacitance of the produced nanocomposite and pure PANI, cyclic voltammetry measurements were performed at different scan rates: 10, 20, 50 and 100 mV•s^{-1}. The corresponding CV spectra of pure PANI (electrolyte: 0.1 M Aniline + 0.5 M H_2SO_4) is shown on Fig. 4. At the intersection of voltammograms in the region of charge and discharge of the electrochemical double layer, from the corresponding values of anodic and cathodic currents densities, the double layer capacity (C_{dl}) of the produced material can be determined, using the following equation [32]:

$$C_{dl} = \frac{di_{cap}}{d\left(\frac{\partial E}{\partial t}\right)} \qquad (1)$$

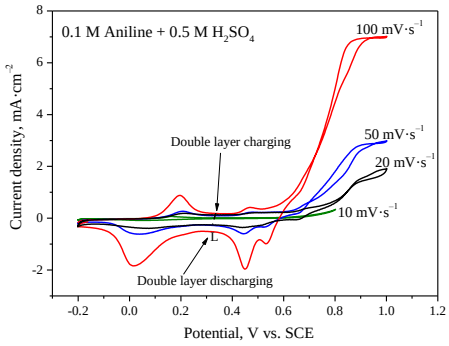

Fig. 4. Cyclic voltammograms of pure aniline (0.1 M aniline + 0.5 M H_2SO_4)at different scanning rates.

The current density of the electrochemical double layer i_{cap} at given scanning rate, is determined as the mean value of the absolute values of the anode and cathode currents at the potential of the intersection of the curves (line L). The dependence of the changes of icapon the scanning rate is a straightline whose slope represents the value of the double layer capacity, C_{dl}.

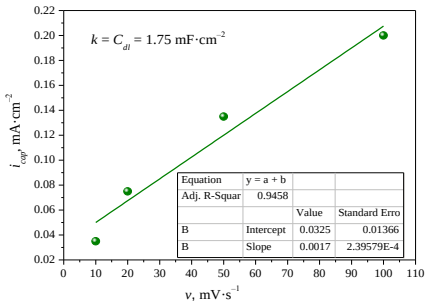

Fig. 5. Dependence of the changes of icap on the scanning rate for the system: 0.1 M Aniline + 0.5 M H_2SO_4.

This is presented in Fig. 5 and the calculated value for the capacity of the polyaniline is 1.75 $mF.cm^{-2}$.

Corresponding voltammogram for the system 0.1 M Aniline + 0.5 M H_2SO_4 + 3 wt. % of chemically modified graphene is shown in Fig. 6.

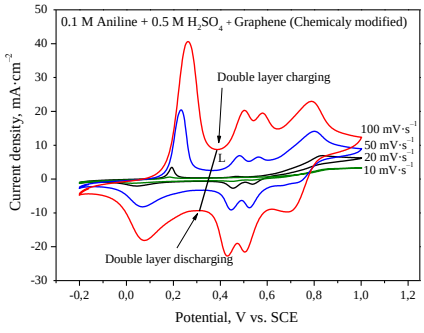

Fig. 6. Cyclic voltammograms of aniline with graphene (0.1 M aniline + 0.5 M H_2SO_4 + graphene 3 % wt.) at different scanning rates.

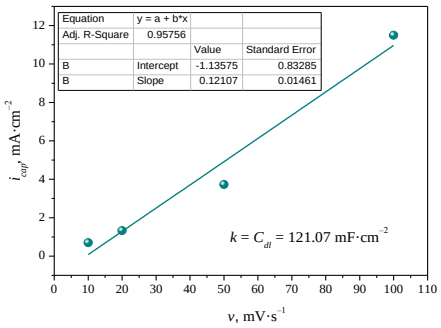

Fig. 7. Dependence of the changes of icap on the scanning rate for the system: 0.1 M Aniline + 0.5 M H_2SO_4 + graphene 3 % wt.

The calculated value for the double layer capacity of the polyaniline/graphene nanocomposite is 121.07 $mF.cm^{-2}$ (Fig. 7).

The double layer capacity increased for about 70 times in relation to the double layer capacity of the pure polyaniline. These results show that by incorporating of only 3 % chemically modified graphene in the polymer matrix, the electrochemical properties of the material can be improved up to several times. This is promising for application of these nanocomposites in electrochemical and energy storage devices [33-35].

3.3. Steady-state polarization measurements

As shown, nanocomposites which consist of PANI/graphene possess enhanced electrical properties. Several authors presented various effects of the graphene on the properties of the polymer matrix [36-39], and all point out that emeraldine's conductive form of PANI is the most appropriate for electrochemical applications and electronic devices. This research is done in order to obtain nanocomposite for sensing applications. Therefore, the produced material should have good electrical properties. In our previous work [40], steady-state polarization measurements have shown that PANI as emeraldine form can be produced at constant potentials in the region of 0.64–0.8 V. But, the optimal potential in electrolyte that contains 0.1 M Aniline + 0.5 M H_2SO_4 + graphene, was shown to be 0.75 V [40].

In this work, steady-state galvanostatic measurements were performed in order to determine the influences of different electrolysis conditions on the electro-polymerization of PANI/graphene nanocomposites at constant potential of 0.75 V.

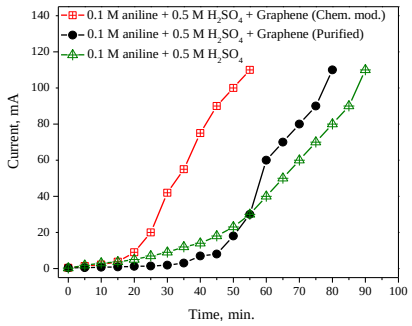

Fig. 8. Steady-state polarization curves for pure aniline and aniline with addition of differently treated graphene.

Firstly, the influence of purification and modification of graphene to the polymerization rate was studied. This is shown in Figure 8. The system with purified graphene at the beginning shows slower polymerization rate when compared to that of pure PANI, but later, the polymerization rate increases. Also, the change of current is non- linear until 60 mA, at which the nanocomposite was already formed, and further on the current shows linear changes. This is due to the wrinkled and folded structure of graphene as result of the purification process, which causes non-uniform forming of the polymer chains on the graphene surface [22]. This can be explained by the so called induction period [41-43], when embryos are created. Also, several successive processes of polymer chain formation occur such as oxidation of aniline to radical cations, oxidation of these radicals to oligomers and finally, forming of a macromolecule of PANI. After forming of the macromolecule of PANI, the polymerization process is stabilized [44]. This also confirms that graphene acts as an incipient in the electro-polymerization process, but that purification does not have much effect on the polymerization rate. By performing the chemical modification process of the graphene surface, a faster rate of polymerization is achieved and the linearity of the curve is more uniform. The polymerization rate is almost double than pure PANI. This shows that chemical modification of the graphene surface causes much better and stable conductivity than that of purified CNSs, due to the carboxyl and hydroxyl groups which allows better interactions with polymer matrix [45]. This is in accordance with the results of SEM/EDS and CV analysis.The influence of the mass fraction of graphene (1, 2, 3 and 10 % wt.) in the polymer matrix on electro-polymerization rate is shown in Figure 9 [46]. As can be seen, the electron exchange is faster with increasing the mass fraction of the nanofiller. This is result of increasing of electrical conductivity of the nanocomposite.

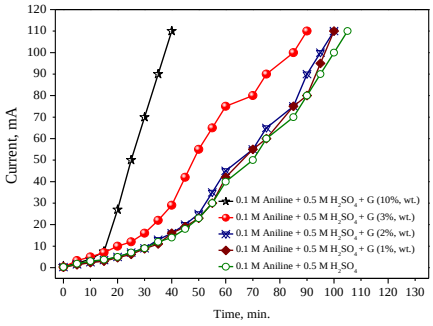

Fig. 9. Steady-state polarization curves for aniline with addition of different quantity of graphene.

Finally, two different pathways of introducing the graphene in the polymer matrix and their impact on the rate of polymerization were studied. The first pathway was introducing the graphene in PANI matrix through it previously being deposited on a platinum electrode, and subsequently PANI being deposited on a graphene film. The second pathway was introducing the graphene in the electrolyte and their mutual depositing with PANI on the platinum electrode. These results are shown in Figure 9. As it can be seen, the polymerization rate of the nanocomposites is higher when the nanostructure was previously deposited on a platinum electrode. This is attributed to the larger active surface area created on the platinum electrode, due to the presence of graphene [47, 48]. In contrary, when graphene was introduced in the electrolyte, the polymerization rate is lower, due to the fact that an induction period is necessary at first, to create a rough surface which would have a role of incipient and would initiate the polymerization process. Related to this, from the morphological aspect of the nanocomposites, using a first pathway of introducing the CNSs in the polymer matrix, a layer by layer structure is created, and the benefits of the carbon nanostructure do not come to the fore. Using the second pathway, when the CNSs are introduced in the electrolyte, compact nanocomposite with uniform distribution of CNSs trough the PANI matrix is produced, and a better material is obtained [5].

4. CONCLUSIONS

The investigations in this study were motivated by the idea to produce PANI/graphene nanocomposites by electrochemical polymerization, aimed for application in the manufacturing of sensors. The influences of the different process conditions were examined. According to the

presented results, the following conclusions can be drawn:

1. According to SEM/EDS analysis, purification of the graphene with H_2O_2 and HF leads to a wrinkled structure that causes sheet folding, while modification with strong acid solutions (H_2SO_4 + HNO_3), leads to edges cutting and gives more uniform form of the flakes. Also, the observed oxidized edges at the graphene flakes can be attributed to the formation of some amide and carbamide groups with hydroxyl and carboxyl groups. This is useful for application of graphene in some electrochemical devices.

2. CV measurements have shown that the presence of graphene in the electrolyte intensifies the growth of the nanocomposite on the electrode. Graphene acts as an incipient in the system because of its large specific surface area and accelerates the reaction rate. Incorporation of only 3 % chemically modified graphene in the polymer matrix, can improve the electrochemical behavior of the system (current density – electro-polymerization rate) up to several times.

3. Steady state polarization measurements confirmed that graphene acts as an incipient in the electro-polymerization process, but that purification does not have a great effect on the polymerization rate. The chemical modification of the CNSs surface have shown higher and more uniform polymerization rate and the polymerization rate is almost double than pure PANI. This also confirms that chemical modification of the graphene surface, improves the conductivity and stability of the material better than only purified graphene. This is due to the carboxyl and hydroxyl groups which allows better interactions with the polymer matrix and confirms previously stated conclusions from SEM/EDS and CV analysis.

4. From the results, the impact of graphene on the electrical conductivity of the nanocomposites can also be assessed. And here confirmed is that by increasing the graphene mass fraction from 1%, 2%, 3% up to 10 %, the electron exchange becomes faster, thus increasing the electrical conductivity of the nanocomposite.

5. Through analyzing the different pathways of introduction of graphene in the polymer matrix and their impact on the polymerization rate, it has been confirmed that the polymerization rate of the nanocomposites is greater when the nanostructure is previously deposited on a platinum electrode.

Acknowledgements: *This research was performed under the FP7 Project COMMON SENS - "Cost-effective sensors, interoperable with international existing ocean observing systems to meet EU policies requirements" (Project reference 614155).*

REFERENCES

1. H. S. Nalwa, Handbook of Organic Conductive Molecules and Polymers. Wiley, New York, 1–4, 1997.
2. E. Hermelin, J. Petitjean, S. Aeiyach, J. C. Lacroix, P. C. Lacaze, *J. App. Electrochem*., **31**, 905 (2001).
3. C. H. Chen, *J. Appl. Polym. Sci*., **89**, 2142 (2003).
4. M. Angelopoulos, R. Dipietro, W. G. Zheng, A. G. MacDiarmid, A. J. Epstein, *J Synth Met.*, **84**, 35 (1997).
5. R. Ansari, M. B. Keivani, *E-J Chem*., **3**, 202 (2006).
6. J. Huang, S. Virji, B. Weiller, R. B. Kaner, *Chem. A Eur. J*., **10**, 1314 (2004)
7. H. Pingsheng, Q. Xiaohua, L. Chune, *Synth. Met.*, **57**, 5008 (1993).
8. K. G. Neoh, E. T. Kang, S. H. Khor K. L Tan, *Polym. Deg. Stab.*, **27**, 107 (1990).
9. M. Angelopoulos, A. Ray, A. G. Macdiarmid, A. J. Epstein, *J. Synth. Met*., **21**, 21 (1987).
10. G. M. Morales, M. C. Miras, C. Barbero, *Synth. Met.*, **101**, 686 (1996).
11. S. H. Kim, J. H. Seong, *J. Appl. Polym. Sci*., **83**, 2245(2002).
12. P. Gajendran, R. Saraswathi, *Pure Appl. Chem.*, **80**, 2377 (2008).
13. B. Lakard, G. Herlem, S. Lakard, R. Guyetant, *Polym.*, **46**, 12233 (2005).
14. N. Liu, F. Luo, H. Wu, Y. Liu, C. Zhang, Y. Chen, *Adv. Funct. Mate*r., **18**, 1518 (2008).
15. T. Wei, G. Luo, Z. Fan, C. Zheng, J. Yan, C. Yao, W. Li, C. Zhang, *Carbon*, **4**7, 2296 (2009).
16. C. Schwandt, T. A. Dimitrov, J. D. Fray, *J. of Electroanal. Chem.*, **647**,150 (2010).
17. C. Panatarani, N. Muthahhari, A. Rianto, J. M. Joni, *AIP Conf. Proc*.**, 1719**, 030022 (2016).
18. E. Bekyarova, M. E. Itkis, P. Ramesh, C. Berger, M. Sprinkle, W. A. de Heer, R. C. Haddon, *J. Am. Chem. Soc.*, **131**, 1336 (2009).
19. M. Alanyahoğlu, J J. Segura, J. Oró-Solè, N. Casañ-Pastor, *Carbon*, **50**, 142 (2012).
20. Z. Yanwu, M. Shanthi, C. Weiwei, L. Xuesong, J. W. Suk, R. J. Poots, R. S. Ruoff, *Adv. Mat*., **22**, 3906 (2010).
21. J. Xie, J. P. Spallas, *Micros. and Microanal*.,**19** , 370 (2013).
22. H. Zhang, P. X. Feng, *Carbon*, **48**, 359 (2010).
23. D. W. Boukhvalov, M. I. Katsnelson, *Nano Lett*., **8**, 4373 (2008).
24. A. S. Mildvan, M. C. Scrutton, M. F. Utter. *J. Bio.l Chem.*, **241**, 3488 (1996).
25. C. E. Bowen, E. Rouscher, L. L. Ingraham, *Arch. Biochem Biophy*s., **125**, 865 (1968).
26. S. Pruneanu, E. Veress, I. Marian, L. Oniciu, *J. Mater. Sci.*, **34**, 2733 (1999).
27. K. H. Hassan, N. F. Atta, A., *Int. J. Electrochem. Sci.*, **7**, 11161 (2012).
28. J. Gu, S. Kan, Q. Shen, J. Kan, *Int. J. Electrochem. Sci.*, **9**, 6858 (2014).

29. B. O. Taranu, E. Fagadar-Cosma, I. Popa, N. Plesu, I. Taranu, *Digest J. Nanomat. and Biostruct.*, **9**, 667 (2014).
30. E. Genies, M. Lapkowski, J. Penneau, *J. Electroanal. Chem. Interfac. Electrochem.*, **249**, 97 (1988).
31. J. Q. Dong, Q. Shen, *J. Polym. Sci. Part B: Polym. Phys.*, **47**, 2036 (2009).
32. L. M. Da Silva, L. A. De Faria, J. F. C. Boodts, *Electrochim. Acta*, **4**7, 395 (2001).
33. C. Peng, S. Zhang, D. Jewell, G. Z. Chen, *Prog. Nat. Sci.*, **18**, 777 (2008).
34. J. Zheng, H. Ma, X. He, M. Gao, G. Li, *Procedia Eng*., **27**, 1478 (2012).
35. A. Kumar, V. Kumar, K. Awasthi, *J. of Polym. Plastics. Techn. and Eng.*, **57**, 70 (2017).
36. A. O. Al-Hartomy, A. A. Al-Ghamdi, A. S. F. Al Said, N. Dishovsky, R. Shtarkova, V. Iliev, *Appl. Polym. Comp*., **2**, 59 (2014).
37. J. Zhu, H. Gu, Z. Luo, N. Haldolaarachige, D. P. Young, S. Wei, Z. Guo, *Langmuir*, **28**, 10246 (2012).
38. O. K. Park, N. H. Kim, G. H. Yoo, K. Y. Rhee, J. H. Lee, *Comp. Part. B: Eng*., **41**, 2 (2010).
39. J. C. García-Gallegos, I. Martín-Gullón, J. A. Conesa, Y. I. Vega-Cantú, F. J. Rodríguez-Macías, *Nanotech*., **2**7, 015501 (2016).
40. A. Petrovski, P. Paunović, R. Avolio, M. E. Errico, M. Cocca, G. Gentile, A. Grozdanov, M. Avella, J. Barton, T. A. Dimitrov, *Mat. Chem. Phys*., **185**, 83 (2017).
41. H. Yang, A. Bard, *J. Electroanal. Chem*., **339**, 423 (1997).
42. S. Mu, J. Kan, J. Lu, L. Zhuang, *J. Electroanal. Chem.*, **446**,107 (1998).
43. A. Malinauskas, J. Malinauskienė, *CHEMIJA*, **16**, 1 (2005).
44. N. Gospodinova, L. Terlemezyan, *Prog. Polym. Sci*., **23**, 1443 (1998).
45. S. Niyogi, E. Bekyarova, M. E. Itkis, J. L. McWilliams, M. A. Hamon, R. C. Haddon, *J. Am. Chem. Soc*., **128**, 7720 (2006).
46. N. H. Alamusi, F. Hisao, A. Satoshi, L. Yaolu, L. Jinhua, *Sens*., **11**, 10691 (2011).
47. E. N. Konyushenko, J. Stejskal, M. Trchová, J. Hradil, J. Kovářová, J. Prokeš, M. Cieslar, J. Y. Hwang, K. H. Chen, I. Sapurina, *Polym*., **47**, 5715 (2006).
48. Y. K. Zhou, B. L. He, W. J. Zhou, H. L. Li, *J. Electrochem. Soc.*, **151**, 1052 (2004).